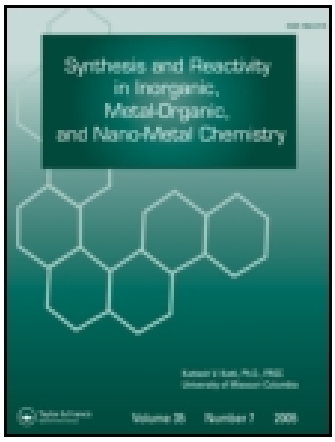

Synthesis and Reactivity in Inorganic, Metal-Organic, and Nano-Metal Chemistry

Publication details, including instructions for authors and subscription information:
http://www.tandfonline.com/loi/lsrt20

Nucleolytic Property Promoted by Biologically Active Metal-Based Complexes Formed by Neutral Quatridentate Ligands: Synthesis, Characterization, and DNA Binding Studies

K. Pothiraj [a] , T. Baskaran [a] & N. Raman [a]

[a] Research Department of Chemistry , VHNSN College , Virudhunagar , India

Accepted author version posted online: 12 Jul 2012.Published online: 28 Aug 2012.

To cite this article: K. Pothiraj , T. Baskaran & N. Raman (2012) Nucleolytic Property Promoted by Biologically Active Metal-Based Complexes Formed by Neutral Quatridentate Ligands: Synthesis, Characterization, and DNA Binding Studies, Synthesis and Reactivity in Inorganic, Metal-Organic, and Nano-Metal Chemistry, 42:8, 1192-1203, DOI: 10.1080/15533174.2012.684262

To link to this article: http://dx.doi.org/10.1080/15533174.2012.684262

Synthesis and Reactivity in Inorganic, Metal-Organic, and Nano-Metal Chemistry, 42:1192–1203, 2012

ISSN: 1553-3174 print / 1553-3182 online
DOI: 10.1080/15533174.2012.684262

Taylor & Francis
Taylor & Francis Group

Nucleolytic Property Promoted by Biologically Active Metal-Based Complexes Formed by Neutral Quatridentate Ligands: Synthesis, Characterization, and DNA Binding Studies

K. Pothiraj, T. Baskaran, and N. Raman
Research Department of Chemistry, VHNSN College, Virudhunagar, India

A series of Ni(II), Cu(II), and Zn(II) complexes have been synthesized and characterized with physicochemical and spectral techniques. Absorption titration study of the interaction of the complexes with calf-thymus (CT) DNA has shown that the complexes can bind to CT DNA. The cyclic voltammograms of all the complexes recorded in the presence of CT DNA-buffer solution have shown that they can bind to CT DNA *via* intercalation mode, which has also been verified by the viscosity experiments. The antimicrobial and DNA cleavage activities of all the compounds have also been investigated.

Keywords antimicrobial activity, DNA binding, metal complexes, nucleolytic property

INTRODUCTION

Schiff base is an organic compound in which the nitrogen atom of an amino group is double bonded to a carbon atom. The Schiff base acts as an electron sink that greatly stabilizes negative charge that develops on the adjacent carbon. The chelating structures, moderate electron donation, and easy tunable electronic and steric effects proved Schiff bases to be flexible ligands capable of stabilizing different metals in various oxidation states with unusual structural features.[1,2] Characteristic Schiff base provides geometrical cavity control for host–guest interaction and modulation of its lipophilicity offers remarkable selectivity, sensitivity, and stability for a specific metal ion.

Recent works have shown a growing interest in the interaction of small molecules/metal complexes with DNA.[3,4] The design of DNA and RNA specific agents capable of controlled chemical cleavage are of paramount importance due to their potential use as drugs, regulators of gene expression, and tools for molecular biology.[5] Metal complexes are attractive reagents for the cleavage of nucleic acids due to their inherently diverse structure and reactivity. Several studies have been carried out on the complexes that cleave DNA through an oxidative pathway which requires a coreactant such as an oxidizing or reducing agent, light, or redox-active metal center in addition to the principal cleavage agent.[6,7]

In recent years, the interest concerning copper(II) complexes has been focused on complexes containing Schiff bases derived from ketones and diamines.[8,9] This group of complexes has been studied due to their antimicrobial and anticancer activities. Complexes breaking double-stranded DNA duplex are thought to be biologically significant sources of cell lethality, because they appear to be less readily repaired by DNA repair mechanisms. The potential applications of metal complexes as non-radioactive probes of nucleic acid structure and possible DNA cleaving agents have been explored extensively.[10,11] In these complexes, the metal or ligands can be varied in an easily controlled way to facilitate the individual applications. Copper is a bioessential element with relevant oxidation states. Because of its chemical and biological relevance, a large number of copper(II) complexes have been synthesized and investigated for their pharmacological properties.[12,13]

Very few numbers of Schiff base metal complexes of 2′-methylacetoacetanilide and their derivatives have been reported to possess interesting biological properties such as antitumor, antioxidant, antimicrobial activities, and laboratory uses and many industrial applications.[14] A literature search reveals that the Schiff bases derived from 2′-methylacetoacetanilide and ethylenediamine/phenylenediamine have not been reported. Our interest in the present study deals with the synthesis and spectroscopic characterization of nickel(II), copper(II), and zinc(II) complexes with symmetrical neutral quatridentate (tetradentate) ligands derived from 2′-methylacetoacetanilide and diamines. The investigation of the biological properties of metal complexes has been focused on (a) the binding properties with

Received 13 December 2011; accepted 1 April 2012.
The authors express their heartfelt thanks to the College Managing Board, Principal and Head of the Department of Chemistry, VHNSN College, for providing necessary research facilities. Instrumental facilities provided by Sophisticated Analytical Instrumention Facility (SAIF), IIT Bombay, for EPR spectra and CDRI, Lucknow, for mass spectra and CHN analyses are gratefully acknowledged.
Address correspondence to N. Raman, Research Department of Chemistry, VHNSN College, Virudhunagar 626001, India. E-mail: drn_raman@yahoo.co.in

calf-thymus (CT) DNA performed with electronic absorption spectroscopy, cyclic voltammetry, and viscosity measurements; (b) the study of the nucleolytic activity of the complexes; and (c) the examination of the antimicrobial activity of the ligands as well as their complexes.

EXPERIMENTAL

Materials and General Methods

All chemicals and reagents were of reagent grade quality. Ethylenediamine and phenylenediamine (SD Fine Chemicals, India) and 2′-methylacetoacetanilide (Aldrich, USA) were used as received. The AR grade of $NiCl_2{\cdot}6H_2O$, $CuCl_2.2H_2O$ and $ZnCl_2$ were used. Tris-HCl buffer was purchased from Himedia (Mumbai, India). The supercoiled (SC) pUC19 DNA was purchased from Bangalore Genie, India. CT-DNA, 3-mercaptopropionic acid (MPA), bromophenol blue, xylene cyanol, agarose (molecular biology grade), and ethidium bromide (EB) were obtained from Sigma Aldrich (USA). Tris–HCl buffer was prepared using deionized and sonicated triple-distilled water.

Carbon, hydrogen, and nitrogen analysis of the ligands and their complexes were carried out on a CHN analyzer Carlo Erba 1108 (USA). The infrared spectra (4000–400 cm^{-1} KBr discs) of the samples were recorded on FT-IR Affinity-I spectrophotometer (Shimadzu, Japan). The electronic absorbance spectra (200–1100 nm) were recorded on a UV-1601 spectrophotometer (Shimadzu, Japan). Proton nuclear magnetic resonance spectra were obtained with a 300 MHz Bruker Avance DRX-300 FT-NMR spectrometer (New York, USA). Chemical shifts (ppm) were referenced either with an internal standard (Tetramethylsilane) or to the residual solvent peaks. EPR spectra of complexes in solid state at 300 K and in frozen DMSO at 77 K were recorded on a Varian E–112 spectrometer (United Kingdom) at X-band, using a TCNE as marker with 100 kHz modulation frequency and 9.1 GHz microwave frequency. Mass spectrometry experiments were performed on a JEOL-AccuTOF JMS-T100LC mass spectrometer (USA) equipped with a custom-made electrospray interface (ESI). Molar conductance of 10^{-3} M solution of the complexes in N,N′-dimethylformamide (DMF) was measured at room temperature with an Deep Vision Model-601 digital direct reading deluxe conductivity meter (India). Magnetic susceptibility measurements were carried out by employing the Gouy method at room temperature on powder sample of the complex. $CuSO_4{\cdot}5H_2O$ was used as calibrant. The metal contents of the complexes were determined according to the literature method.[15]

Synthesis of the Ligands and Their Complexes

Preparation of Schiff Base Ligands

The ethanolic solution of ethylenediamine (0.60 g, 10 mmol) or phenylenediamine (1.08 g, 10 mmol) was added to 2′-methylacetoacetanilide (3.82 g, 20 mmol) hot ethanolic solution (Scheme 1). The mixture was refluxed with magnetic stirrer for 3 h and evaporated to room temperature. The product was filtered off and washed with small amount of dilute ethanol and petroleum ether. Recrystallization was carried out in hot ethanol and a yellow-colored amorphous compound was obtained, which was subsequently dried over anhydrous $CaCl_2$ under vacuum.

For $C_{24}H_{30}N_4O_2$ (L_1), Yield (%): 68.38, pale yellow, M.pt: 198°C, M.Wt: 406.52, Anal. Calcd. (%): C, 70.91; H, 7.44; N, 13.78. Found (%): C, 70.85; H, 7.41; N, 13.74; ^{1}H NMR (DMSO-d_6, δ/ppm): 8.67 (2H, –NH), 7.02–7.71 (8H, Ar–H), 3.36 (4H,C–CH_2C–), 2.86 (12H, –CH_3), 1.71–2.32 (4H, –CH_2–CH_2); IR (KBr, ν/cm^{-1}): 3211 ν(NH), 3065 ν(Ar–CH), 2984,2945 ν(aliphatic–CH), 1651 ν(–CONH), 1612 ν(C=N), 1548 ν(Ar–C=C); UV–Vis (λ_{max}/ nm) (DMF): 265 and 310.

For $C_{28}H_{30}N_4O_2$ (L_2): Yield (%): 66.95, yellow, M.pt: 211°C, M.Wt: 454.57, Anal. Calcd. (%): C, 73.98; H, 6.65; N, 12.33. Found (%): C, 73.94; H, 6.62; N, 12.28; ^{1}H NMR (DMSO-d_6, δ/ppm): 8.70 (2H, –NH), 6.96–7.83 (12H, Ar–H), 3.41 (4H, C–CH_2C–), 2.94 (12H, –CH_3)); IR (KBr, ν/cm^{-1}): 3232 ν(NH), 3058 ν(Ar–CH), 2991,2939 ν(aliphatic–CH), 1658 ν(–CONH), 1619 ν(C=N), 1552 ν(Ar–C=C); UV–Vis (λ_{max}/ nm) (DMF): 270 and 325.

Preparation of Nickel(II), Copper(II), and Zinc(II) Complexes

$NiCl_2.6H_2O$ (0.237 g; 1.0 mmol) or $CuCl_2.2H_2O$ (0.170 g; 1.0 mmol) or $ZnCl_2$ (0.136 g; 1.0 mmol) dissolved in ethanol was slowly added to Schiff base ligand L_1 (0.406 g; 1.0 mmol) / L_2 (0.454 g; 1.0 mmol) dissolved in hot ethanol and refluxed for 2 h. The resulting colored solution was concentrated to approximately 5 mL, thereby a colored precipitate was formed. It was filtered, washed with ethanol, and dried *in vacuo*.

For $[NiC_{24}H_{30}N_4O_2Cl_2]$ ($[NiL_1Cl_2]$): Yield (%): 70.73, green, M.pt: >250°C, M.Wt: 536.12, Anal. Calcd. (%): Ni, 10.95; C, 53.77; H, 5.64; N, 10.45; Cl, 13.23. Found (%): Ni, 10.91; C, 53.75; H, 5.60; N, 10.42; Cl, 13.21; IR (KBr, ν/cm^{-1}): 3215 ν(–NH), 3064 ν(Ar–CH), 2985, 2944 ν(aliphatic–CH), 1637 ν(C=O),1594 ν(C=N), 1551 ν(Ar–C=C), 578 ν(Cu–O), 486 ν(Cu–N); UV–Vis (λ_{max}/nm) (DMF): 268, 321, 583, 762, and 960. Molar conductance (DMF): 7.11 ohm^{-1} cm^2 mol^{-1}; μ_{eff} (BM): 3.06.

For $[CuC_{24}H_{30}N_4O_2Cl_2]$ ($[CuL_1Cl_2]$): Yield (%): 73.47, light green, M.pt: >250°C, M.Wt: 540.97, Anal. Calcd. (%): Cu, 11.75; C, 53.29; H, 5.59; N, 10.35; Cl, 13.11. Found (%): Cu, 11.69; C, 53.24; H, 5.56; N, 10.32; Cl, 13.09; IR (KBr, ν/cm^{-1}): 3213 ν(–NH), 3067 ν(Ar–CH), 2983, 2945 ν(aliphatic–CH), 1635 ν(C=O),1599 ν(C=N), 1549 ν(Ar–C=C), 585 ν(Cu–O), 493 ν(Cu–N); UV–Vis (λ_{max}/nm) (DMF): 270, 323, 670, and 767; molar conductance (DMF): 8.58 ohm^{-1} cm^2 mol^{-1}; μ_{eff} (BM): 1.79.

For $[ZnC_{24}H_{30}N_4O_2Cl_2]$ ($[ZnL_1Cl_2]$): Yield (%): 71.86, yellow, M.pt: >250°C, M.Wt: 542.82, Anal. Calcd. (%): Zn, 12.05; C, 53.10; H, 5.57; N, 10.32; Cl, 13.06. Found (%): Zn, 12.01; C, 53.08; H, 5.53; N, 10.29; Cl, 13.03; ^{1}H NMR (DMSO-d_6, δ/ppm): 8.69 (2H, –NH), 7.03–7.75 (12H, Ar–H),

3.37 (4H, C–CH_2C–), 2.89 (12H, –CH_3), 1.72–2.35 (4H, –CH_2–CH_2); IR (KBr, ν/cm^{-1}): 3215 ν(–NH), 3068 ν(Ar–CH), 2984, 2947 ν(aliphatic–CH), 1639 ν(C=O),1597 ν(C=N), 1550 ν(Ar–C=C), 573 ν(Cu–O), 497 ν(Cu–N); UV–Vis (λ_{max}/nm) (DMF): 269 and 331; molar conductance (DMF): 9.23 ohm^{-1} cm^2 mol^{-1}; μ_{eff} (B.M.): Diamagnetic.

For [$NiC_{28}H_{30}N_4O_2Cl_2$] ([NiL_2Cl_2]): Yield (%): 69.04, red, M.pt: >250°C, M.Wt: 584.17, Anal. Calcd. (%): Ni, 10.05; C, 57.57; H, 5.18; N, 9.59; Cl, 12.14. Found (%): Ni, 10.03; C, 57.52; H, 5.14; N, 9.56; Cl, 12.00; IR (KBr, ν/cm^{-1}): 3236 ν(–NH), 3059 ν(Ar–CH), 2988, 2943 ν(aliphatic–CH), 1641 ν(C=O),1601 ν(C=N), 1552 ν(Ar–C=C), 569 ν(Cu–O), 452 ν(Cu–N); UV–Vis (λ_{max}/nm) (DMF): 277, 334, 595, 774, and 987. molar conductance (DMF): 10.85 ohm^{-1} cm^2 mol^{-1}; μ_{eff} (BM): 3.11.

For [$CuC_{28}H_{30}N_4O_2Cl_2$] ([CuL_1Cl_2]): Yield (%): 71.62, brown, M.pt: >250°C, M.Wt: 589.02, Anal. Calcd. (%): Cu, 10.79; C, 57.10; H, 5.13; N, 9.51; Cl, 12.04. Found (%): Cu, 10.73; C, 57.06; H, 4.97; N, 9.48; Cl, 12.01; IR (KBr, ν/cm^{-1}): 3235 ν(–NH), 3060 ν(Ar–CH), 2989, 2941 ν(aliphatic–CH), 1639 ν(C=O),1596 ν(C=N), 1553 ν(Ar–C=C), 572 ν(Cu–O), 458 ν(Cu–N); UV–Vis (λ_{max}/nm) (DMF): 274, 339, 694, and 789; molar conductance (DMF): 12.69 ohm^{-1} cm^2 mol^{-1}; μ_{eff} (BM): 1.84.

For [$ZnC_{28}H_{30}N_4O_2Cl_2$] ([ZnL_1Cl_2]): Yield (%): 70.58, yellow, M.pt: >250°C, M.Wt: 590.87, Anal. Calcd. (%): Zn, 11.07; C, 56.92; H, 5.12; N, 9.48; Cl, 12.00; Found (%): Zn, 11.03; C, 56.90; H, 5.08; N, 9.46; Cl, 11.97; ^{1}H NMR (DMSO-d_6, δ/ppm): 8.71 (2H, –NH), 6.97–7.86 (12H, Ar–H), 3.44 (4H, CH_2), 2.96 (12H, –CH_3); IR (KBr, ν/cm^{-1}): 3234 ν(–NH), 3059 ν(Ar–CH), 2992, 2940 ν(aliphatic–CH), 1644 ν(C=O),1603 ν(C=N), 1552 ν(Ar–C=C), 580 ν(Cu–O), 455 ν(Cu–N); UV–Vis (λ_{max}/nm) (DMF): 280 and 346; molar conductance (DMF): 11.77 ohm^{-1} cm^2 mol^{-1}; μ_{eff} (B.M.): Diamagnetic.

DNA Interaction Studies

Absorption Titration

The DNA binding experiments were performed in Tris–HCl buffer (50 mM Tris HCl/5 mM NaCl buffer, pH 7.2). The concentration of CT DNA was determined by measuring the absorption intensity at 260 nm with ε value of 6600 M^{-1} cm^{-1}.[16] Absorption titration experiments were made using different concentrations of CT DNA, keeping the concentration of the complexes constant, with due correction for the absorbance of the CT DNA itself. Samples were equilibrated before recording each spectrum. To compare quantitatively the affinity of the complexes bound to DNA, the intrinsic-binding constants K_b of the complexes were obtained by monitoring the changes in absorbance with increasing concentration of DNA using the following equation:[17]

$$[DNA]/(\varepsilon_a - \varepsilon_f) = [DNA]/(\varepsilon_b - \varepsilon_f) + 1/K_b(\varepsilon_b - \varepsilon_f) \quad [1]$$

where [DNA] is the concentration of DNA in base pair, and ε_a, ε_f, and ε_b correspond to the apparent absorption coefficient A_{obsd}/[M], the extinction coefficient for the free complex, and the extinction coefficient for the complex in the fully bound form, respectively.

Cyclic Voltammetry

Cyclic voltammetry studies were performed on a CH Instrument Electrochemical analyzer. Cyclic voltammetry experiments were carried out in a 15 mL three-electrode electrolytic cell. The working electrode was glassy carbon, a platinum wire was used as the counter electrode and an Ag/AgCl electrode saturated with KCl was used as the reference electrode. The cyclic voltammograms of the complexes were recorded in (1:2) DMF:buffer solutions at v = 100 mV s^{-1} where Tris-HCl buffer and 0.1 M Bu_4NClO_4 solution were used as the supporting electrolytes. Oxygen was removed by purging the solutions with pure nitrogen that had been previously saturated with solvent vapors. All electrochemical measurements were performed at 25°C.

Viscometric Measurements

Viscometric studies were done using a Ubbelodhe viscometer, thermostated at 37°C in a constant temperature bath. The concentration of DNA was kept constant in all samples, but the complex concentration was varied and the flow time for each sample was measured three times. An average flow time was calculated. The data were presented as $(\eta/\eta_0)^{1/3}$ versus binding ratio (R = [complex]/[DNA]), where η is the viscosity of DNA in the presence of the complex and η_0 is that of DNA alone. Viscosity values were calculated from the observed flowing time of DNA containing solutions (t) corrected for that of the buffer alone (t_0): $\eta = (t - t_0)/t_0$.

DNA Cleavage and Mechanism Studies

For the gel electrophoresis analysis, the supercoiled pUC19 DNA (30 μM, 0.2 μg) was treated with complexes in presence of 3-mercaptopropionic acid in 50 mM Tris–HCl/5 mM NaCl, buffer (pH 7.2). The solution was then incubated for 1 h at 37°C, then a quench buffer solution containing bromophenol blue (0.25%) and sucrose (40%) was added. In the ensuing step, samples were immediately loaded on 0.8% agarose gel for electrophoresis in Tris-acetate-EDTA (TAE) buffer (pH 8.0) containing 1.0 μg/mL EB at 50 V for 2 h. Finally, the gel was photographed under UV light. Cleavage mechanistic investigation of pUC19 DNA was carried out in the presence of standard radical scavengers. These reactions were carried out by adding standard radical scavengers such as ethanol (EtOH), sodium azide (NaN_3), and superoxide dismutase (SOD) to pUC19 DNA prior to the addition of complex. Cleavage was initiated by the addition of complex and quenched with 2 μL of loading buffer. Further analysis was carried out by the previous standard method.

Determination of Antimicrobial Activity

Paper Disc Method

Sterilized discs were used. Fresh stock solutions (1 mg/mL) of the synthesized compounds were prepared in redistilled dimethylsulfoxide (DMSO) according to the required concentrations.[18] The discs were impregnated in DMSO. Each disc was impregnated with 0.1 mL DMSO and so the total amount of compound contained in each disc was 100 μg. The media for bacteria and fungi were nutrient agar and dextrose agar respectively. Media was prepared and sterilized by autoclaving for 15 min at 121°C, then the medium was cooled to 50°C inoculated with the previously prepared bacteria suspension and poured in sterilize Petri dishes. The medium was allowed to solidify after a simple circular movement of the plates. Paper discs previously impregnated with the solution of compounds to be tested were placed on the plates. The plates were then incubated for 24 h at 37°C in case of bacteria and 48 h at 37°C in case of fungi. On each plate an appropriate reference antibiotic disc was applied depending on the test microorganisms. To ensure that the solvent had no effect on bacterial and fungi growth, a control test was performed with test medium supplemented with DMSO following the same procedure as given in the experiment. DMSO showed no inhibition zones.

Dilution Method

To determine the MIC for the all the compounds dilution method[19] was used. The compounds were dissolved and then diluted using DMSO, twofold serial concentrations of the compounds were employed to determine the MIC ranging from 200 to 0.78 μg/mL. The MIC value was determined as the lowest concentration of the compound that completely inhibited macroscopic growth of microorganism.

RESULTS AND DISCUSSION

The results of the elemental analysis of ligands L_1 and L_2 and their Ni(II), Cu(II), and Zn(II) complexes were recorded and are given in Experimental section. All the metal complexes are colored, non-hygroscopic, and are quite stable at room temperature. They are found to be insoluble in common organic solvents such as methanol, ethanol, dichloromethane, and acetonitrile, except DMF and DMSO. The molar conductance data of the complexes in DMF at 10^{-3} M is in the range 7.11–12.69 ohm^{-1} cm^2 mol^{-1}, which indicates non-electrolytic nature of the complexes suggesting that the chloride anions are coordinated to metal ion. Different attempts such as crystallization using mixtures of solvents and low-temperature crystallization were unsuccessful to obtain a single crystal suitable for X-ray crystallography. However, the analytical, spectral, and magnetic data enable us to expect the possible structure of the prepared complexes.

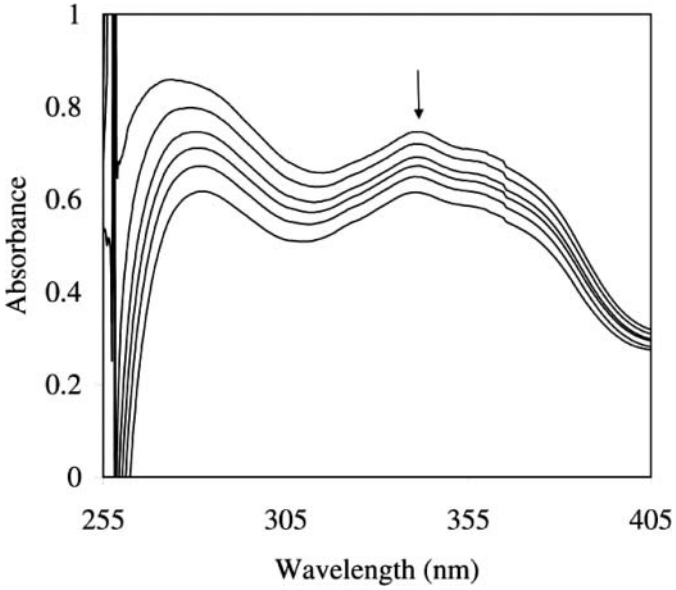

FIG. 1. Absorption spectrum of $[CuL_2Cl_2]$ in the absence and presence of increasing amounts of CT DNA at room temperature in 50 mM Tris-HCl/5 mM NaCl buffer (pH 7.2). Arrow shows the absorbance changing upon increasing DNA concentration.

Electronic Absorption Spectra and Magnetic Moment

The electronic spectra of the free ligands (L_1 and L_2) exhibit two bands in the range of 265–270 and 310–325 nm, assigned to $\pi \rightarrow \pi^*$ transition of aromatic rings and azomethine groups, respectively (Figures 1 and 2). The electronic spectra of $[CuL_1Cl_2]$ and $[CuL_2Cl_2]$ complexes (Figures 3 and 4) show a broad band centered at 670–694 and 767–789 nm, which are attributed to $^2B_{1g} \rightarrow {}^2E_{1g}$ and $^2B_{1g} \rightarrow {}^2A_{1g}$ transitions characterized by copper(II) ion in octahedral geometry.[20] The octahedral geometry of copper(II) ion in the above mentioned copper(II) complexes is confirmed by the measured magnetic moment values in the range 1.79–1.84 B.M. which is in harmony with the reported value. The proposed octahedral geometry around the nickel(II) ion is also confirmed by the position of absorption bands appeared at 960, 762, and 583 nm for $[NiL_1Cl_2]$ and 987, 774, and 595 nm for $[NiL_2Cl_2]$ complexes, attributed to $^3A_{2g}(F) \rightarrow {}^3T_{2g}(F)$, $^3A_{2g}(F) \rightarrow {}^3T_{1g}(F)$ and $^3A_{2g}(F) \rightarrow {}^3T_{1g}(P)$ transitions, respectively. The magnetic moment values of 3.06 and 3.11 B.M. are observed for $[NiL_1Cl_2]$ and $[NiL_2Cl_2]$, respectively, corresponding to an octahedral environment around the nickel(II) ion.

Infrared Spectra of the Ligands and Their Metal Complexes

The infrared spectra provided valuable information regarding the nature of the functional groups attached to the metal atom. The intense band in the region 1612–1619 cm^{-1} in the IR spectra of free Schiff base ligands is associated with C=N stretching vibration and is shifted to lower frequencies

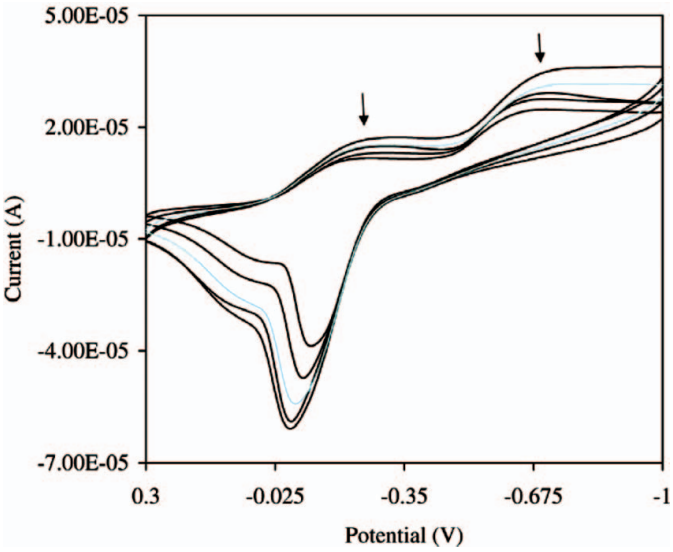

FIG. 2. Cyclic voltammagram of $[CuL_2Cl_2]$ in the absence and presence of increasing amounts of CT DNA at room temperature in DMF:buffer (1:2) mixture (pH 7.2). Arrow shows the current changing upon increasing DNA concentration (color figure available online).

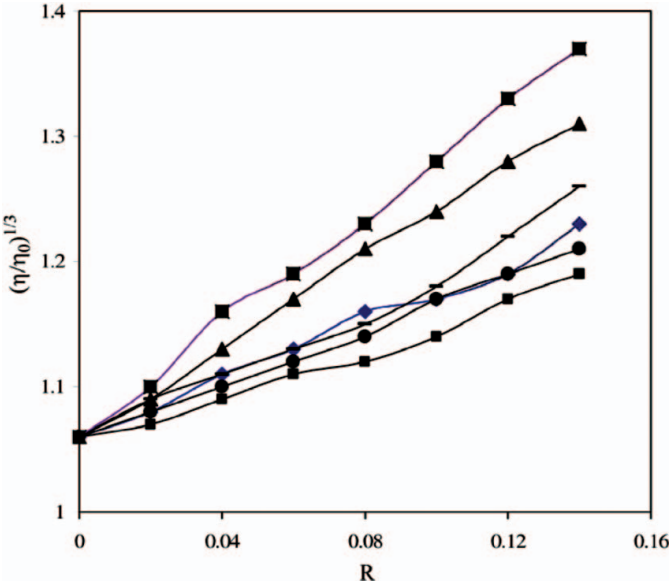

FIG. 3. Effect of increasing amounts of $[CuL_2Cl_2]$ (■), $[CuL_1Cl_2]$ (▲), $[NiL_2Cl_2]$ (−), $[NiL_1Cl_2]$ (♦), $[ZnL_2Cl_2]$ (●), and $[ZnL_1Cl_2]$ (■) on the relative viscosity of CT DNA versus the [complex]/[DNA] (R) ratio (color figure available online).

(1594–1603 cm^{-1}) in the spectra of corresponding metal complexes. This indicated the coordination of imine nitrogen to the metal ion.[21] It was noted that in the infrared spectra of the ligands as well as all the complexes, a single medium intensity band in the region 3211–3232 cm^{-1} is present, which may be assigned to the ν(N–H) stretching vibration of amide moiety of 2′-methylacetoacetanilide. The absorption bands at 1651–1658 cm^{-1} due to ν(C=O) stretching frequencies of amide moiety, in the free ligands shift towards lower values (1635–1644 cm^{-1}) in the spectra of the complexes of Ni(II), Cu(II), and Zn(II) ions. This behavior indicates the fact that the carbonyl oxygen atom of the 2′-methylacetoacetanilide residue was coordinated. The infrared spectra of all the metal complexes reveal that (M-O) and (M-N) stretching vibrations are in the range 452–497 cm^{-1} and 569–585 cm^{-1}, respectively.

Proton Nuclear Magnetic Resonance Spectra

The Schiff bases and their zinc complexes have been characterized by proton nuclear magnetic resonance spectra to ensure the ligands and their zinc complexes purity in solution and elucidate the differently positioned protons. The NMR spectra of the Schiff base ligands L_1 and L_2, the singlet signals ranging at 8.67–8.70, 3.36–3.41, and 2.86–2.94 ppm are ascribed to -NH (2H) protons of the amide moiety of the 2′-methylacetoacetanilide, C-CH_2-C (4H) proton, and aromatic and aliphatic protons of -CH_3 (12H), respectively. In addition to this the multiplet signals around the ranges at 7.02–7.71 and 6.96–7.83 ppm are due to aromatic protons of L_1 and L_2, respectively. A characteristic triplet signal at 1.71–2.32 ppm is assigned to CH_2-CH_2 (4H) protons of ligand L_1. In the case of diamagnetic zinc complexes, all the signals are slightly shifted

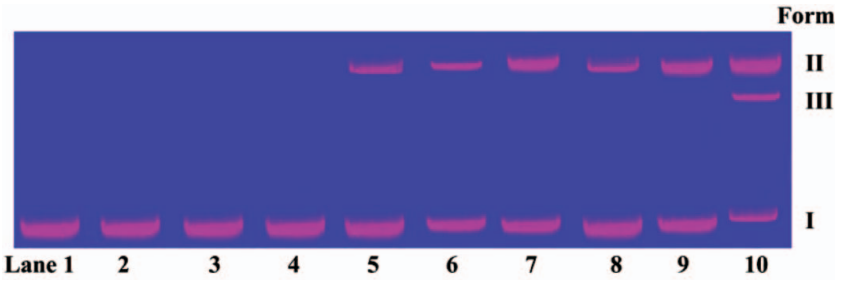

FIG. 4. Gel electrophoresis diagram showing the cleavage of supercoiled pUC19 DNA (0.2 μg) in 50 mM Tris–HCl/5 mM NaCl buffer (pH 7.2) incubated at 37°C for 2 h with different concentrations of copper complexes in the presence of MPA (100 μM) as an reducing agent: Lane 1, Control DNA; Lane 2, DNA + MPA; Lane 3, DNA + $[CuL_1Cl_2L]$ (30 μM); Lane 4, DNA + $[CuL_2Cl_2]$ (30 μM); Lane 5, DNA + MPA + $[CuL_1Cl_2]$ (30 μM); Lane 6, DNA + MPA + $[CuL_1Cl_2]$ (60 μM); Lane 7, DNA + MPA + $[CuL_1Cl_2]$ (100 μM); Lane 8, DNA + MPA + $[CuL_2Cl_2]$ (30 μM); Lane 9, DNA + MPA + $[CuL_2Cl_2]$ (60 μM); Lane 10, DNA + MPA + $[CuL_2Cl_2]$ (100 μM) (color figure available online).

to high value of δ, which reveals that the coordination takes place and the data of the complexes are given in the experimental part.

Mass Spectra

The mass spectrum has been successfully used to examine molecular species in solution. The pattern of the mass spectrum gives an impression of the successive degradation of the target compound with the series of peaks corresponding to the various fragments. In the present investigation the ESI-mass spectra of L_1, L_2, and $[CuL_2Cl_2]$ have been recorded and show a molecular ion peak at m/z = 406, 455, and 589, respectively, which corresponds to the molecular weight of the respective ligands (L_1 and L_2) and the copper complex of L_2 ($[CuL_2Cl_2]$) and also copper complex shows ^{35}Cl isotopic peaks observed at 591 (M+2) and 593 (M+4). The fragmentation of $[CuL_2Cl_2]$ gives the elimination of two chloride ions followed by the demetallation and the m/z values are 520 (M-1) and 454 which corresponds to the fragment ions $[CuC_{28}H_{30}N_4O_2]^{+\cdot}$ and $[C_{28}H_{30}N_4O_2]^{+\cdot}$, respectively. Also, some other unstable fragments are observed in the same copper complex, and the peaks at m/z = 189, 174, and 148 correspond to the fragment ions $[C_{11}H_{13}N_2O]$, $[C_{10}H_{10}N_2O]$, and $[C_9H_{10}NO]$, respectively. This fragmentation pattern confirms that the complexes have two chloride ions inside the coordination sphere and the complex is monomeric in nature.

EPR Spectral Studies

EPR studies of copper(II) complexes give information about the distribution of the unpaired electrons and hence about the nature of the bonding between the metal ion and its ligand. The X-band EPR spectra of $[CuL_2Cl_2]$ complex was recorded in DMSO solution at liquid nitrogen temperature (LNT) and at room temperature (RT).

In the present work, there is no information obtained from the room temperature EPR spectrum of copper complex. The values of $g_\parallel$ and $g_\perp$ were worked out from the spectra at LNT using tetracyanoethylene (TCNE) free radical as a "g" marker. The ordering of g values [$g_\parallel$ (2.28) > $g_\perp$ (2.05) > g_e (2.0027)] observed for the copper(II) complex indicates that the unpaired electron is localized in $d_{x2\text{-}y2}$ orbital of the copper(II) ion.[22] The value of g_{av} (2.12) was calculated according to the equation $g_{av} = 1/3[g_\parallel + 2\, g_\perp]$.

The axial symmetry parameter G, which is a measure of the exchange interaction between copper centers in the polycrystalline compound, is calculated using Hathaway expression ($G = g_\parallel - 2.0027/\, g_\perp - 2.0027$).[23] According to Hathaway, if the value of G > 4, the exchange interaction is negligible in solid complex but G < 4 indicates considerable interaction in solid complex. In the present case, G value (5.86) > 4, indicating no exchange interaction between the copper(II) centers in DMSO at 77 K.

Electron paramagnetic resonance and optical spectrum have been used to determine the covalent bonding parameters for the copper(II) ion in various environments. Since there has been wide interest in the nature of bonding parameters in the system, we adopted the simplified molecular orbital theory to calculate the molecular orbital coefficients such as α^2 (covalent in-plane σ bonding) and β^2 (covalent in-plane π bonding), which were calculated by using the following equations:[24]

$$\alpha^2 = (A_{||}/0.036) + (g_{||} - 2.0027) + (3/7)(g_\perp - 2.0027) + 0.04 \quad [2]$$

$$\beta^2 = (g_{||} - 2.0027)E_{d-d}/(-8\lambda\alpha^2) \quad [3]$$

If the α^2 value is 0.5, it indicates a complete covalent bonding, while the value of $\alpha^2 = 1.0$ suggests a complete ionic bonding. The observed value of α^2 (0.97) indicates that the complex has covalent character and $\beta^2 = 1.08$, which suggests that in plane π-bonding is also present in the complex. The observed values indicate that there is interaction in the in plane π-bonding, whereas in-plane σ-bonding is completely ionic. This is also confirmed by orbital reduction factors ($K_\parallel$ and $K_\perp$), which are calculated from the following equations:

$$K_{||}^2 = (g_{||} - 2.0027)E_{d-d}/8\lambda \quad [4]$$

$$K_\perp^2 = (g_\perp - 2.0027)\ E_{d-d}/2\lambda \quad [5]$$

where $\lambda = -828$ cm^{-1} for the free metal ion. In the case of pure σ- bonding $K_\parallel = K_\perp$, whereas $K_\parallel < K_\perp$ implies considerable in-plane π-bonding while for out-plane π-bonding $K_\parallel > K_\perp$. For the present complex, the observed order is $K_\parallel$ (0.75) > $K_\perp$ (0.56), implying a greater contribution from out-plane π-bonding than from in-plane π-bonding in metal ligand π –bonding. Based on the previous analytical and spectral data, it is concluded that the copper(II) complex has an octahedral geometry.

Electrochemical Properties of Metal Complexes

The electrochemical properties of the metal(II) complexes have been studied by cyclic voltammetry under nitrogen atmosphere in DMF solution in the potential range +1.0 to 1.5 V versus Ag/AgCl reference and the results are presented in Table 1. The cyclic voltammetry of Ni(II) complexes exhibits both anodic and cathodic redox potentials. In anodic potential region the reduction wave (E_{pc}, –0.248 for $[NiL_1Cl_2]$ and –0.395 V for $[NiL_2Cl_2]$) corresponding to Ni(II)/Ni(I) reaction is obtained. During the reverse scan the oxidation of Ni(I)/Ni(II) occurs in the potential range (Epa, –0.078 for $[NiL_1Cl_2]$ and –0.223 V for $[NiL_2Cl_2]$). The ratio of peak current (Ipc/Ipa) is not equal to one and the values of the limiting peak-to-peak separation ($\Delta Ep = Epa - Epc$) are greater than 0.060 V. Therefore, the redox couple in voltammetric data can be attributed to a quasireversible one-electron transfer process. The cathodic cyclic voltammetry of Cu(II) complexes displays two cathodic peaks in the potential range (Epc^1,–0.249 to –0.584 V and Epc^2,

TABLE 1
Electrochemical behavior of metal(II) complexes in the absence and presence of CT DNA

		E_{pc}(V)		E_{pa}(V)		ΔE_p(V)		$E_{1/2}$(V)	
Complex	Redox couple	Free	Bound	Free	Bound	Free	Bound	Free	Bound
$[NiL_1Cl_2]$	Ni(II)/Ni(I)	–0.248	–0.196	–0.078	–0.029	0.170	0.167	–0.163	–0.112
$[CuL_1Cl_2]$	Cu(II)/Cu(I)	–0.249	–0.224	–0.101	–0.052	0.148	0.172	–0.175	–0.138
	Cu(I)/Cu(0)	–0.709	–0.663	—	—	—	—	—	—
$[ZnL_1Cl_2]$	Zn(II)/zn(I)	–1.096	–1.050	—	—	—	—	—	—
$[NiL_2Cl_2]$	Ni(II)/Ni(I)	–0.395	–0.364	–0.223	–0.201	0.172	0.163	–0.309	–0.283
$[CuL_2Cl_2]$	Cu(II)/Cu(I)	–0.584	–0.571	–0.105	–0.078	0.481	0.493	–0.346	–0.325
	Cu(I)/Cu(0)	–0.725	–0.708	—	—	—	—	—	—
$[ZnL_2Cl_2]$	Zn(II)/Zn(I)	–1.112	–1.093	—	—	—	—	—	—

–0.709 to –0.725 V for $[CuL_1Cl_2]$ and $[CuL_1Cl_2]$, respectively), due to the reduction of Cu(II)–Cu(I) and Cu(I)– Cu(0) couples respectively. In the reverse anodic scan one anodic peak in the potential range (Epa[1], –0.101 V to –0.105 V for $[CuL_1Cl_2]$ and $[CuL_1Cl_2]$), due to the oxidation of Cu(I)–Cu(II) couple. The ratio of peak current (Ipc/Ipa) is less than one and the value of peak-to-peak separation (ΔEp) = 0.148 to 0.481 V, which indicates that the first redox couple for these complexes involved in quasireversible one-electron transfer process, whereas the observed second redox couple is irreversible in nature. The cyclic voltammetry measurement upon scanning cathodically, $[ZnL_1Cl_2]$ and $[ZnL_2Cl_2]$ complexes display an irreversible one-electron peak assigned to the reduction of Zn(II)–Zn(I) at –1.096 and –1.112 V, respectively. The absence of the anodic signal is indicative of a fast chemical reaction following the charge transfer step and instability of the electrochemically generated Zn(I) species, respectively.

Binding Characteristics of Metal Complexes With DNA

The interactions of metal complexes with DNA have been the subject of interest for the development of effective chemotherapeutic agents. Transition metal centers are particularly attractive moieties for such research since they exhibit well-defined coordination geometries and also often possess distinctive electrochemical or photophysical properties, thus enhancing the functionality of the binding agent.[25]

Electronic Absorption Titration

In general, if a small molecule interacts with DNA, changes in absorbance (hypochromism) and in the position of the band (red shift) should occur. This phenomenon indicates that the small molecule has intercalated into DNA base pairs, and is involved in a strong interaction in the molecular stack between the aromatic chromophore and the base pairs. The spectral effects have been rationalized as[26] the empty π^*-orbital of the small molecule couples with the π^*-orbital of the DNA base pairs, which causes an energy decrease, and a decrease of the $\pi-\pi^*$ transition energy. Therefore, the absorption of the small molecule should exhibit a red shift. At the same time, the empty π^*-orbital is partially filled with electrons to reduce the transition probability, which leads to hypochromism.

To achieve this, the electronic absorption spectra of the metal complexes of Schiff base ligands (L_1 and L_2) in the absence and presence of the CT DNA at different concentrations (at a constant concentration of the complexes) were measured (Table 2) and one representative $[CuL_2Cl_2]$ complex is given in Figure 5. In the absorption spectra of $[NiL_1Cl_2]$, $[CuL_1Cl_2]$, $[ZnL_1Cl_2]$, $[NiL_2Cl_2]$, $[CuL_2Cl_2]$, and $[ZnL_2Cl_2]$, the bands centered at

TABLE 2
Absorption titration of metal(II) complexes with CT DNA

	λ_{max}(nm)				
Complex	Free	Bound	$\Delta\lambda$ (nm)	Hypochromicity (%)	$K_b \times 10^3$ (M^{-1})
$[NiL_1Cl_2]$	321.2	321.6	0.4	12.05	2.73
$[CuL_1Cl_2]$	323.0	323.8	0.8	21.30	4.19
$[ZnL_1Cl_2]$	331.4	331.8	0.4	11.76	2.51
$[NiL_2Cl_2]$	334.7	335.3	0.6	15.83	3.12
$[CuL_2Cl_2]$	339.1	340.5	1.4	30.88	7.82
$[ZnL_2Cl_2]$	346.3	346.8	0.5	13.47	2.78

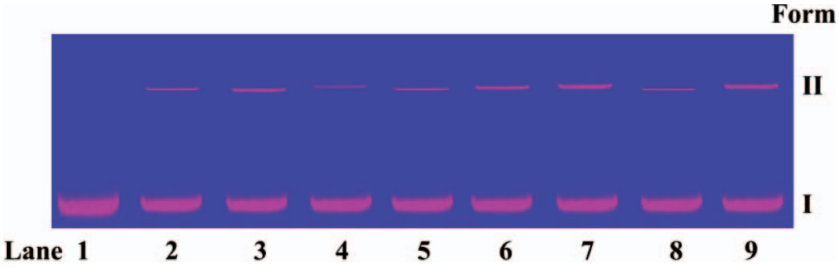

FIG. 5. Gel electrophoresis diagram showing the cleavage of supercoiled pUC19 DNA (0.2 μg) in 50 mM Tris–HCl/5 mM NaCl buffer (pH 7.2) incubated at 37°C for 2 h with two different concentration of zinc and nickel complexes in the presence of MPA (100 μM) as an reducing agent: Lane 1, Control DNA; Lane 2, DNA + MPA + [ZnL_1Cl_2L] (50 μM); Lane 3, DNA + MPA + [ZnL_1Cl_2] (100 μM); Lane 4, DNA + MPA + [ZnL_2Cl_2] (50 μM); Lane 5, DNA + MPA + [ZnL_2Cl_2] (100 μM); Lane 6, DNA + MPA + [NiL_1Cl_2] (50 μM); Lane 7, DNA + MPA + [NiL_1Cl_2] (100 μM); Lane 8, DNA + MPA + [NiL_2Cl_2] (50 μM); Lane 9, DNA + MPA + [NiL_2Cl_2] (100 μM) (color figure available online).

321.2, 323.0, 331.4, 334.7, 339.1, and 346.3 nm exhibit slightly red shift in the range of 0.4–1.4 nm with hypochromism of 12.05%, 21.30%, 11.76%, 15.83%, 30.88%, and 13.47%, respectively. The calculated K_b values of [NiL_1Cl_2], [CuL_1Cl_2], [ZnL_1Cl_2], [NiL_2Cl_2], [CuL_2Cl_2], and [ZnL_2Cl_2] are 2.73×10^3 M^{-1}, 4.19×10^3 M^{-1}, 2.51×10^3 M^{-1}, 3.12×10^3 M^{-1}, 7.82×10^3 M^{-1}, and 2.78×10^3 M^{-1}, respectively. The observed intrinsic DNA binding constants are similar to the values obtained for many reported first row transition metal complexes those show intercalative binding to DNA,[27,28] but much smaller than the classical intercalators and metallointercalators where binding constants reported in the order of 10^7 M^{-1}.[29] From the results, the [CuL_2Cl_2] complex shows higher affinity towards CT-DNA. However from these measurements, it is not clear to conclude that whether DNA binds through an intercalative mode or not. So, further studies are needed to elucidate the exact nature of the binding mode.

DNA Interaction of Electrochemical Studies

The electrochemical investigations of metal–DNA interactions could also provide useful supplement to spectroscopic method and yield information about interactions (electrostatic or intercalative) with the reduced and oxidized forms of the metal. The difference between voltammetric responses of [CuL_2Cl_2] in the absence and presence of CT-DNA is illustrated in Figure 6. The significant shift in peak potentials of metal(II) complexes is observed upon addition of CT-DNA. The summary of voltammetric results for Ni(II), Cu(II) and Zn(II) complexes in the absence and presence of CT-DNA is given in Table 1. No new redox peaks are appeared after the addition of CT DNA to each complex, but the current intensity decreases significantly, suggesting the existence of an interaction between each complex and CT DNA, explained in terms of an equilibrium mixture of free and DNA-bound complex on the electrode surface.[30] In general, the electrochemical potentials of a small molecule will shift positively when it intercalates into DNA double helix, and, if it is bound to DNA by electrostatic interaction, the potential will shift to a negative direction. Additionally, if more potentials than one present such a shift, a positive shift of Epa and a negative shift of Epc may imply that the molecule can bind to DNA by both intercalation and electrostatic interaction.[31]

All the complexes exhibit similar electrochemical behavior upon addition of CT DNA with positive shifts for the cathodic potentials Epc (ΔEpc = +0.052 V for [NiL_1Cl_2],

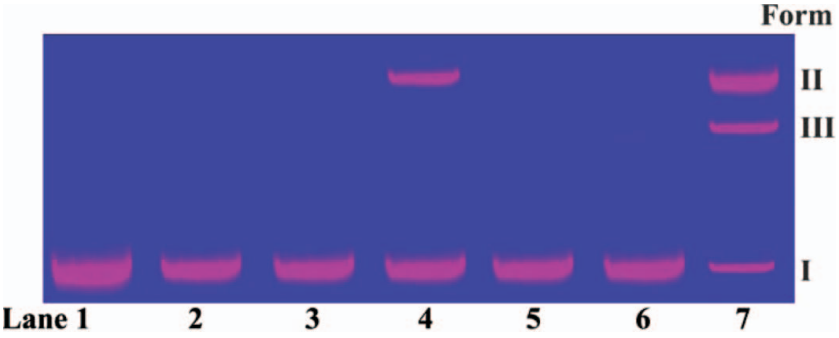

FIG. 6. Gel electrophoresis diagram showing the cleavage of supercoiled pUC19 DNA (0.2 μg) by copper(II) complexes (100 μM) with addition of MPA (100 μM) and radical scavengers in 50 mM Tris–HCl/5 mM NaCl buffer (pH 7.2) and incubated at 37°C for 2 h: Lane 1, DNA control; Lane 2, DNA + MPA + [CuL_1Cl_2] + NaN_3 (100 μM); Lane 3, DNA + MPA + [CuL_1Cl_2] + EtOH (4 μL); Lane 4, DNA + MPA + [CuL_1Cl_2] + SOD (4 Units); Lane 5, DNA + MPA + [CuL_2Cl_2] + NaN_3 (100 μM); Lane 6, DNA + MPA + [CuL_2Cl_2] + EtOH (4 μL); Lane 7, DNA + MPA + [CuL_2Cl_2] + SOD (4 Units) (color figure available online).

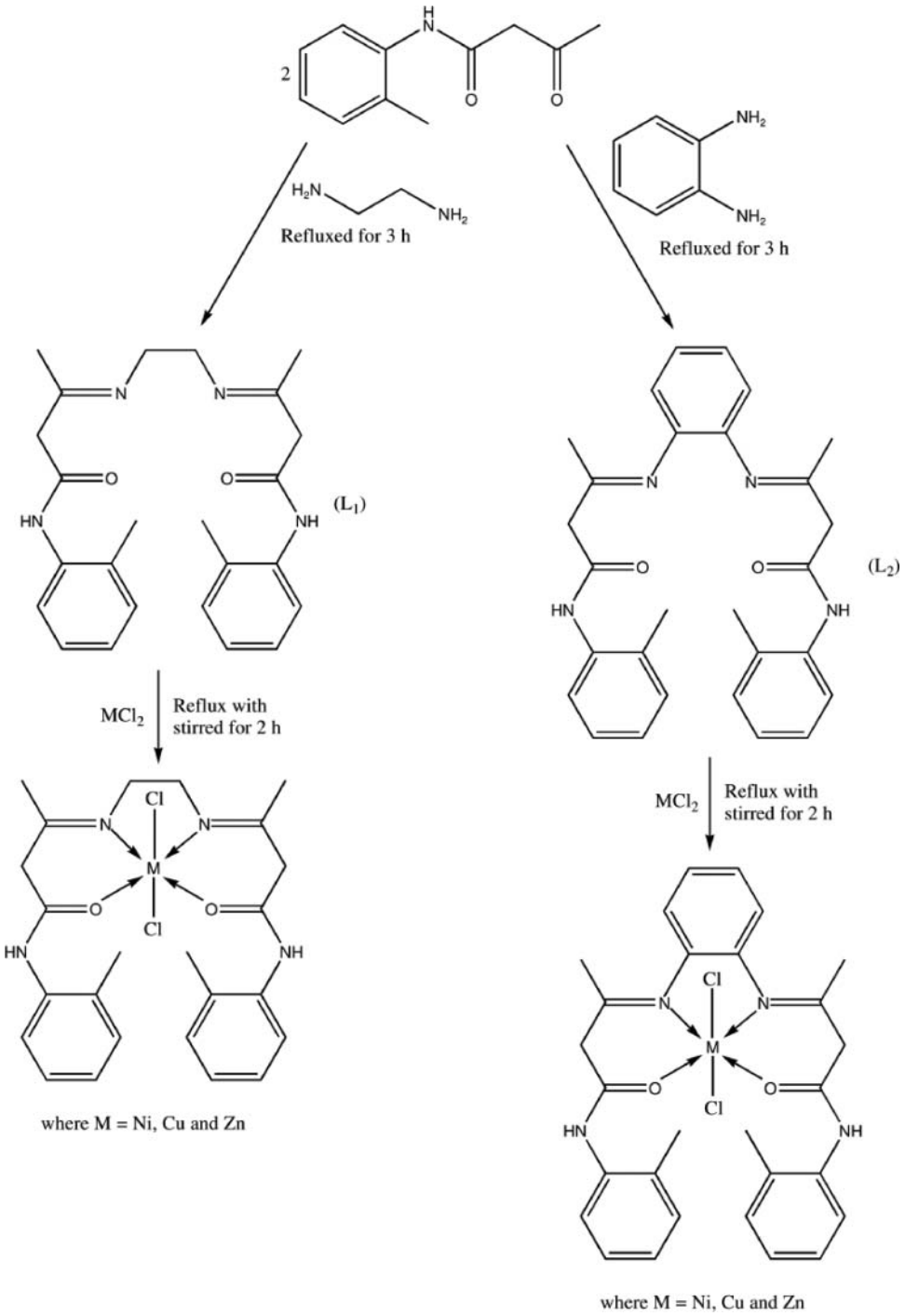

SCH. 1. Outline of the synthesis of ligands and their complexes.

ΔEpc = +0.031 V for $[NiL_2Cl_2]$, ΔEpc^1 = +0.029 V; and ΔEpc^2 = +0.046 V for $[CuL_1Cl_2]$, ΔEpc^1 = +0.016 V and ΔEpc^2 = +0.017 V for $[CuL_2Cl_2]$, ΔEpc = +0.046 V for $[ZnL_1Cl_2]$, and ΔEpc = +0.019 V for $[ZnL_2Cl_2]$, respectively) and also the anodic potentials Epa shift to positive values (ΔEpa = +0.049 V for $[NiL_1Cl_2]$, ΔEpa = +0.021 V for $[NiL_2Cl_2]$, ΔEpa^1 = +0.051 V for $[CuL_1Cl_2]$, and ΔEpa^1 = +0.027 V for $[CuL_2Cl_2]$, respectively). These shifts show that all the complexes could bind to DNA by intercalative interaction.[32] The presence of DNA in the solution at the same concentration of six complexes causes a considerable decrease in the voltammetric current. The drop of the voltammetric

TABLE 3
The *in vitro* antimicrobial activity of ligands and their metal(II) complexes evaluated by minimum inhibitory concentration (μg/mL)

	Antibacterial activity				Antifungal activity			
Compound	*S. aureus*	*B. subtilis*	*E. coli*	*P. aeruginosa*	*A. niger*	*R. bataicola*	*R. stolonifer*	*C. albicans*
L_1	100	100	200	200	100	200	200	200
L_2	100	100	100	200	100	100	200	200
$[NiL_1Cl_2]$	25	12.5	100	50	50	25	100	100
$[CuL_1Cl_2]$	12.5	12.5	25	50	25	25	50	25
$[ZnL_1Cl_2]$	50	25	50	100	25	100	50	50
$[NiL_2Cl_2]$	12.5	25	25	50	12.5	25	50	50
$[CuL_2Cl_2]$	6.25	12.5	12.5	25	6.25	12.5	50	25
$[ZnL_2Cl_2]$	25	25	25	50	25	25	100	50
Ciprofloxacin	0.78	1.56	0.78	1.56	—	—	—	—
Flucanozole	—	—	—	—	0.78	1.56	1.56	1.56

currents in the presence of CT DNA could be attributed to diffusion of the metal complex bound to the large, slowly diffusing DNA molecule. Therefore, the results parallel to the previous absorption spectroscopic titration of metal complexes in the presence of DNA.

DNA-Binding Study with Viscosity Measurements

DNA viscosity is sensitive to DNA length change; therefore, its measurement upon addition of a compound is often concerned as the least ambiguous method to clarify the interaction mode of a compound with DNA and provides reliable evidence for the intercalative binding mode.[33] In the case of classic intercalation, DNA base pairs are separated in order to host the bound compound resulting in the lengthening of the DNA helix and subsequently increase the DNA viscosity. On the other hand, the binding of a compound exclusively in DNA grooves by means of partial and nonclassic intercalation causes a bend or kink in the DNA helix reducing its effective length and, as a result, DNA solution viscosity is decreased or remains unchanged. Viscosity measurements have been carried out on CT DNA solutions upon addition of increasing amounts of metal complexes (Figure 7). The addition of the complexes results in an increase in the relative viscosity of DNA, which may be explained by the insertion of the compounds in between the DNA base pairs, leading to an increase in the separation of base pairs at intercalation sites and, thus, an increase in overall DNA length.[34,35] Thus, the results obtained from the viscosity experiments validate those obtained from the spectroscopic and electrochemical studies.

Nucleolytic Property of Complexes

The study on the cleavage capacity of transition metal complexes to DNA is considerably interesting, as it can contribute to understanding the toxicity mechanism of them and to develop novel artificial nuclease. The cleavage ability of complexes in the presence of reducing agent (3-mercaptopropionic acid) to pUC19 DNA is investigated by gel electrophoresis in Tris-HCl buffer (pH 7.2) at 37°C for 2 h (Figure 8). Control experiments suggest that untreated DNA and DNA incubated with either copper complexes or 3-mercaptopropionic acid do not show any significant DNA cleavage (Lanes 1–4). At low to medium concentration (30–60 μM), both the $[CuL_1Cl_2]$ and $[CuL_2Cl_2]$ complexes show efficient DNA cleavage activity while the $[CuL_2Cl_2]$ complex shows higher cleavage activity than $[CuL_1Cl_2]$ complex in the presence of reducing agent. At the higher concentration (100 μM), the DNA cleavage reaction of $[CuL_1Cl_2]$ complex exhibits the supercoiled form (Form I), which is converted into nicked form (Form II) only but the $[CuL_2Cl_2]$ complex shows the supercoiled form (Form I) is completely converted into nicked form (Form II) and linear form (Form III) due to the complex having higher DNA binding properties. The concentration dependent DNA cleavage property of Ni(II) and Zn(II) complexes (50 μM and 100 μM) in the presence of MPA to pUC19 DNA is studied by gel electrophoresis in Tris-HCl buffer (pH 7.2) at 37°C for 2 h (Figure 9). In different concentrations, the above two Ni(II) and Zn(II) complexes display lower DNA cleavage and therefore the DNA cleavage mechanistic study focuses only on the Cu(II) complexes. In general, copper complexes can cleave DNA through hydrolytic and oxidative processes. For the oxidative process, the complexes have been shown to react with molecular oxygen or hydrogen peroxide to produce a variety of active oxidative intermediates (reactive oxygen species or nondiffusible copper-oxene species). In order to obtain information about the active chemical species that is responsible for the DNA cleavage that occurs in the presence of hydroxyl radical scavengers (EtOH), singlet oxygen quenchers (NaN_3), and superoxide scavenger (SOD) under our experimental conditions. Figure 10 shows that NaN_3 (Lanes 2 and 5) and EtOH (Lanes 3 and 6) significantly

reduce the nuclease activity of the complexes, which is indicative of the involvement of the singlet oxygen and hydroxyl radical in the cleavage process. Further, the addition of SOD (Lanes 4 and 7) has no significant effect on the DNA cleavage. This fact rules out the involvement of the participation of superoxide anion in the DNA cleavage reaction. This fact implies that DNA cleavage reaction by the complexes should be realized by an oxidative cleavage.

Antimicrobial Evaluation of Ligands and Their Complexes

The synthesized neutral quatridentate ligands and their metal complexes have been screened for their antibacterial and antifungal activities. From the antimicrobial screening observation (Table 3), the nickel and zinc complexes show moderate activity against all microorganisms, which is appreciable as compared to the ligands, whereas the copper complexes show higher antimicrobial activity against *S. aureus* and *A. niger* under identical experimental conditions. This enhancement in antimicrobial property is brought about upon complexation that can be related to the increased lipophilicity that powers the rate of entry of molecules into the cell and inertness of certain metal-ligand linkages, which protects the molecule against enzymatic degradation.[36]

REFERENCES

1. Garnovskii, A.D.; Vasilchenko, I.S.; Garnovskii, D.A.; Kharisov, B.I. Molecular design of mononuclear complexes of acyclic Schiff-base ligands. *J. Coord. Chem.* **2009**, *62*, 151–204.
2. Makio, H.; Kashiwa, N.; Fujita, T. FI catalysts: A new family of high performance catalysts for olefin polymerization. *Adv. Synth. Catal.* **2002**, *344*, 477–493.
3. Gao, E.J.; Wang, K.H.; Gu, X.F.; Yu, Y.; Sun, Y.G.; Zhang, W.Z.; Yin, H.X.; Wu, Q.; Zhu, M.C.; Yan, X.M. A novel binuclear palladium complex with benzothiazole-2-thiolate: Synthesis, crystal structure and interaction with DNA. *J. Inorg. Biochem.* **2007**, *101*, 1404–1409.
4. Selvakumar, B.; Rajendiran, V.; Maheswari, P.; Stoeckli-Evans, H.; Palaniandavar, M. Structures, spectra, and DNA-binding properties of mixed ligand copper(II) complexes of iminodiacetic acid: the novel role of diimine co-ligands on DNA conformation and hydrolytic and oxidative double strand DNA cleavage. *J. Inorg. Biochem.* **2006**, *100*, 316–330.
5. Pyle, A.M.; Barton, J.K. Probing nucleic acids with transition metal complexes. In *Progress in Inorganic Chemistry: Bioinorganic Chemistry*, Lippard, S.J., Ed.; New York: Wiley, **1990**; Vol. 38, pp. 413–475.
6. Sigman, D.S.; Mazumder, A.; Perrin, D.M. Chemical nucleases. *Chem. Rev.* **1993**, *93*, 2295–2316.
7. Burrows, C.J.; Rokita, S.E. Recognition of guanine structure in nucleic acids by nickel complexes. *Acc. Chem. Res.* **1994**, *27*, 295–301.
8. Valent, A.; Melník, M.; Hudecová, D.; Dudová, B.; Kiväkas, R.; Sunberg, M.R. Copper(II) salicylideneglycinate complexes as potential antimicrobial agents. *Inorg. Chim. Acta* **2002**, *340*, 15–20.
9. Valent, A.; Kohutova, M.; Svajlenova, O.; Hudecova, D.; Olejníkova, P.; Melník, M. *N*-salicylidene-*L*-glutamatocopper(II) complexes and their antimicrobial effects. *J. Coord. Chem.* **2004**, *57*, 1279–1285.
10. Cowan, J.A. Chemical nucleases. *Curr. Opin. Chem. Biol.* **2001**, *5*, 634–642.
11. Ji, L.N.; Zou, X.H.; Liu, J.G. Shape- and enantioselective interaction of Ru(II)/Co(III) polypyridyl complexes with DNA. *Coord. Chem. Rev.* **2001**, 216–217, 513–536.
12. Singh, A.P.; Kaushik, N.K.; Verma, A.K.; Hundal, G.; Gupta, R. Synthesis, structure and biological activity of copper(II) complexes of 4-(2-pyridylmethyl)-1,7-dimethyl-1,4,7-triazonane-2,6-dione and 4-(2-pyridylethyl)-1,7-dimethyl-1,4,7-triazonane-2,6-dione. *Eur. J. Med. Chem.* **2009**, *44*, 1607–1614.
13. Berners-Price, S.J.; Johnson, R.K.; Giovenella, A.J.; Faucette, L.F.; Mirabelli, C.K.; Sadler, P.J. Antimicrobial and anticancer activity of tetrahedral, chelated, diphosphine silver(I) complexes: comparison with copper and gold. *J. Inorg. Biochem.* **1988**, *33*, 285–295.
14. Raman, N.; Pothiraj, K.; Baskaran, T. DNA interaction, antimicrobial, electrochemical and spectroscopic studies of metal(II) complexes with tridentate heterocyclic Schiff base derived from 2′-methylacetoacetanilide. *J. Mol. Struct.* **2011**, *1000*, 135–144.
15. Angellici, R.J. *Synthesis and Techniques in Inorganic Chemistry*; Philadelphia: W. B. Saunders, **1969**.
16. Reichmann, M.E.; Rice, S.A.; Thomas, C.A.; Doty, P. A further examination of the molecular weight and size of desoxypentose nucleic acid. *J. Am. Chem. Soc.* **1954**, *76*, 3047–3053.
17. Wolfe, A.; Shimer, G.H. Jr.; Meehan, T. Polycyclic aromatic hydrocarbons physically intercalate into duplex regions of denatured DNA. *Biochem.* **1987**, *26*, 6392–6396.
18. Collins, C.H.; Lyre, P.M.; Grange, J.M. *Microbiological Methods, 6th edn.*; London: Butterworths, **1989**.
19. Jones, R.N.; Barry, A.L.; Gaven, T.L.; Washington, J. A. In *Manual of Clinical Microbiology,* 4th edn., Lennette, E.H.; Balows, A.; Shadomy W.J. (Eds.); Washington, DC: American Society for Microbiology, **1984**.
20. Lever, A.B. P. *Inorganic Electronic Spectroscopy,* 2nd edn.; Amsterdam: Elsevier, **1984**.
21. Meghdadi, S.; Mereiter, K.; Amirnasr, M.; Fadaee, F.; Amiri, A. Synthesis, crystal structure, and electrochemistry of $[Co\{(Me\text{-}sal)_2dien\}(N_3)]$ and $[Co\{(Me\text{-}sal)_2dpt\}(N_3)]$. *J. Coord. Chem.* **2009**, *62*, 734–744.
22. Speir, G.; Csihony, J.; Whalen, A.M.; Pierpont, C.G. Studies on aerobic reactions of ammonia/3,5-Di-tert-butylcatechol Schiff-Base condensation products with copper, copper(I), and copper(II). Strong copper(II)−radical ferromagnetic exchange and observations on a unique N−N coupling reaction. *Inorg. Chem.* **1996**, *35*, 3519–3524.
23. Hathaway, B.J. A new look at the stereochemistry and electronic properties of complexes of the copper(II) ion. *Struct. Bond.* **1984**, *57*, 55–118.
24. Fenton, D.E. *Biocoordination Chemistry*. Oxford, England: Oxford University Press, **1995**.
25. Metcalfe, C.; Thomas, J.A. Kinetically inert transition metal complexes that reversibly bind to DNA. *Chem. Soc. Rev.* **2003**, *32*, 215–224.
26. Long, E.C.; Barton, J.K. On demonstrating DNA intercalation. *Acc. Chem. Res.* **1990**, *23*, 271–273.
27. Ghosh, K.; Kumar, P.; Tyagi, N.; Singh, U.P.; Goel, N. Synthesis, structural characterization and DNA interaction studies on a mononuclear copper complex: nuclease activity via self-activation. *Inorg. Chem. Commun.* **2011**, *14*, 489–492.
28. Manikandamathavan, V.M.; Kavitha, M.; Uma, V.; Parameswari, R.P.; Vasanthi, H.R.; Unni Nair, B. Cytotoxic copper(II) complex of tripyridoquinoxaline with DNA hydrolase activity. *Polyhedron* **2011**, *30*, 1604–1611.
29. Cory, M.; McKee, D.D.; Kagan, J.; Henry, D.W.; Miller, J.A. Design, synthesis, and DNA binding properties of bifunctional intercalators. Comparison of polymethylene and diphenyl ether chains connecting phenanthridine. *J. Am. Chem. Soc.* **1985**, *107*, 2528–2536.
30. Hirohama, T.; Kuranuki, Y.; Ebina, E.; Sugizaki, T.; Arii, H.; Chikira, M.; Selvi, P.T.; Palaniandavar, M. Copper(II) complexes of 1,10-phenanthroline-derived ligands: studies on DNA binding properties and nuclease activity. *J. Inorg. Biochem.* **2005**, *99*, 1205–1219.
31. Psomas, G. Mononuclear metal complexes with ciprofloxacin: Synthesis, characterization and DNA-binding properties. *J. Inorg. Biochem.* **2008**, *102*, 1798–1811.
32. Jiao, K.; Wang, Q.X.; Sun, W.; Jian, F.F. Synthesis, characterization and DNA-binding properties of a new cobalt(II) complex: $Co(bbt)_2Cl_2$. *J. Inorg. Biochem.* **2005**, *99*, 1369–1375.

33. Li, D.; Tian, J.; Gu, W.; Liu, X.; Yan, S. A novel 1,2,4-triazole-based copper(II) complex: Synthesis, characterization, magnetic property and nuclease activity. *J. Inorg. Biochem.* **2010**, *104*, 171–179.
34. Dimiza, F.; Papadopoulos, A.N.; Tangoulis, V.; Psycharis, V.; Raptopoulou, C.P.; Kessissoglou, D.P.; Psomas, G. Biological evaluation of non-steroidal anti-inflammatory drugs-cobalt(II) complexes. *Dalton Trans.* **2010**, *39*, 4517–4528.
35. Dimiza, F.; Perdih, F.; Tangoulis, V.; Turel, I.; Kessissoglou, D.P.; Psomas, G. Interaction of copper(II) with the non-steroidal anti-inflammatory drugs naproxen and diclofenac: synthesis, structure, DNA- and albumin-binding. *J. Inorg. Biochem.* **2011**, *105*, 476–489.
36. Raman, N.; Raja, S.J.; Sakthivel, A. Transition metal complexes with Schiff-base ligands: 4-aminoantipyrine based derivatives: a review. *J. Coord. Chem.* **2009**, *62*, 691–709.